

## Three -Pion Correlations

---

### Minoru Biyajima\*

*Department of Physics, Shinshu University, Matsumoto 390-8621, Japan*

*E-mail: biyajima@azusa.shinshu-u.ac.jp*

### Takuya Mizoguchi

*Toba National College of Maritime Technology, Toba 517-8501, Japan*

*E-mail: mizoguti@toba-cmt.ac.jp*

### Naomichi Suzuki

*Department of Comprehensive Management, Matsumoto University, Matsumoto 390-1295, Japan*

*E-mail: suzuki@matsu.ac.jp*

First of all, we mention the situation of empirical analyses on 3rd order BEC (Bose-Einstein Correlation) at RHIC. Second, we introduce several theoretical formulae / approaches. Third we present our analyses of data in Au+Au at 130 GeV by STAR and preliminary data in Au+Au at 200 GeV by PHENIX Collaborations. Our results also contain analyses by means of core-halo model. Finally, we estimate that the volume of interaction in Au + Au collisions at 130 GeV is  $500 \text{ fm}^3$ , which is compared with  $V = R_{\text{long}}R_{\text{out}}R_{\text{side}} \sim 300 \text{ fm}^3$  in Pb + Pb collision at 2.76 TeV by ALICE Collaboration. Moreover, usefulness of empirical analyses on  $(2\pi^+)\pi^-$  and  $(2\pi^-)\pi^+$  combinations at RHIC and LHC energies is remarked.

*The Seventh Workshop on Particle Correlations and Femtoscopy*

*September 20 - 24 2011*

*University of Tokyo, Japan*

---

\*Speaker.

## 1. Situation of Empirical analyses on 3rd order BEC in Au+Au collision at RHIC

As shown in Table 1, STAR and PHENIX Coll. have reported their analyses at 130 GeV and 200 GeV, respectively. In their analyses, STAR Coll. [1] used all combinations of three momentum-transfers  $\sqrt{q_{ij}^2} \leq Q_3$  (Inside of a globe in Fig. 1),

$$Q_{inv,3}^2 = q_{12}^2 + q_{23}^2 + q_{31}^2. \quad (1.1)$$

On the other hand, PHENIX Coll. [2] used data on diagonal line of a cube in Fig. 1,

$$q_3 = \langle q_{12} \rangle = \langle q_{23} \rangle = \langle q_{31} \rangle \quad \text{i.e.} \quad Q_{inv,3}^2 = 3q_3^2. \quad (1.2)$$

Of course this relation holds, as the number of data increases.  $\langle \dots \rangle$  is an average value.

**Table 1:** Situation of analyses on the 3rd order BEC. Notice two empty columns.

$\sqrt{s_{NN}}$	STAR	PHENIX
130 GeV	raw and corrected data by $Q_{inv}$	
200 GeV		preliminary raw and corrected data by $q_3$

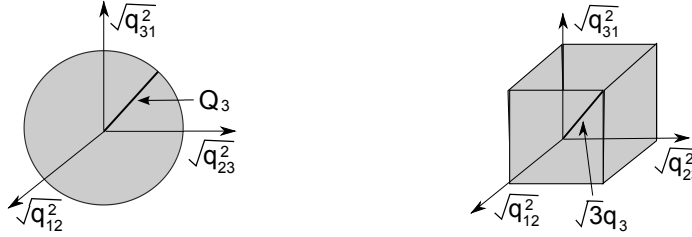


**Figure 1:** Data ensembles of STAR (left) and PHENIX Coll (right).

Here we compare two kinds of data. In Figs. 2, data by PHENIX Coll. are rearranged by  $\sqrt{3}q_3$ . Coincidence among data by STAR and PHENIX Coll is fairly good. Error bars in raw data by PHENIX Coll are smaller than those of STAR Coll.

## 2. Several theoretical formulae

In many analyses on BEC, the following formulae based on plane wave function are used.

$$N^{(2\pi)}/N^{BG} = c \left[ 1 + \lambda e^{-(RQ)^2} \right], \quad (2.1)$$

$$N^{(3\pi)}/N^{BG} = c \left[ 1 + \lambda \sum_{i>j} e^{-(RQ_{ij})^2} + 2\lambda^{1.5} e^{-0.5(RQ_3)^2} \right]. \quad (2.2)$$

In laser optical (LO/GL) approach, the following formulae with a degree of chaoticity  $p$  have been proposed [3] and utilized,

$$N^{(2\pi)}/N^{BG} = 1 + 2p(1-p)E_{2B} + p^2E_{2B}^2, \quad (2.3)$$

$$N^{(3\pi)}/N^{BG} = 1 + 6p(1-p)E_{3B} + 3p^2(3-2p)E_{3B}^2 + 2p^3E_{3B}^3, \quad (2.4)$$

where  $E_{2B}^2 = \exp(-R^2Q^2)$  (Gaussian form) and/or  $E_{2B}^2 = \exp(-R\sqrt{Q^2})$  (exponential form), and  $E_{3B}^3 = \exp(-R^2Q_3^2)$  and so on.

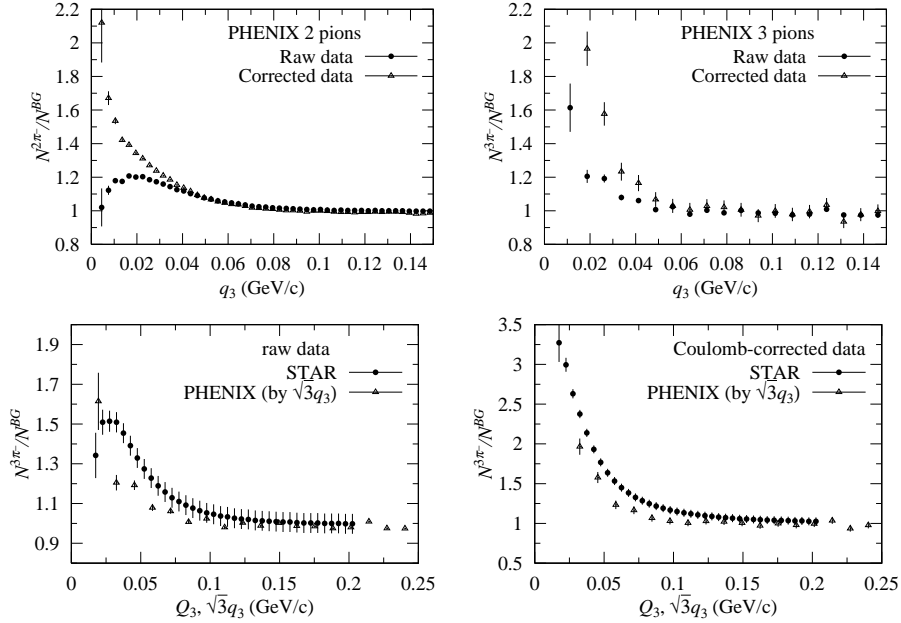


**Figure 2:** Comparisons of data by STAR and PHENIX Coll.

Third we explain the formulae by Coulomb wave function including the degree of coherence  $\lambda$  and the interaction range  $R$  [4, 5, 6, 7]. The two-body Coulomb wave function is well known as,

$$\psi_{k_i k_j}^C(x_i x_j) = \Gamma(1 + i\eta_{ij}) e^{\pi\eta_{ij}/2} e^{ik_{ij}\cdot r_{ij}} F[-i\eta_{ij}, 1; i(k_{ij}r_{ij} - k_{ij}\cdot r_{ij})], \quad (2.5)$$

where,  $r_{ij} = x_i - x_j$ ,  $k_{ij} = (k_i - k_j)/2$ ,  $r_{ij} = |r_{ij}|$ ,  $k_{ij} = |k_{ij}|$  and  $\eta_{ij} = e_i e_j \mu_{ij} / k_{ij}$ .  $\mu_{ij}$ : reduced mass of  $m_i$  and  $m_j$ ,  $F[a, b; x]$ : confluent hypergeometric function,  $\Gamma(x)$ : Gamma function.

Using of Eq. (2.5), the 2nd order BEC with  $\lambda$  and Gaussian form for  $\rho(x_i)$  is calculated as,

$$\begin{aligned} N^{(2\pi^-)} &= \frac{1}{2} \prod_{i=1}^2 \int \rho(x_i) d^3 x_i |\psi_{k_1 k_2}^C(x_1, x_2) + \psi_{k_1 k_2}^C(x_2, x_1)|^2 \\ &= \prod_{i=1}^2 \int \rho(x_i) d^3 x_i \left[ \frac{1}{2} (|\psi_{k_1 k_2}^C(x_1, x_2)|^2 + |\psi_{k_1 k_2}^C(x_2, x_1)|^2) \right. \\ &\quad \left. + \lambda \text{Re} \left( \psi_{k_1 k_2}^C(x_1, x_2) \psi_{k_1 k_2}^{C*}(x_2, x_1) \right) \right], \end{aligned} \quad (2.6)$$

The 3rd order BEC is computed based on the 3-body Coulomb wave function in [6],

$$\Psi_f = \psi_{k_1 k_2}^{C'}(x_1, x_2) \psi_{k_2 k_3}^{C'}(x_2, x_3) \psi_{k_3 k_1}^{C'}(x_3, x_1), \quad (2.7)$$

Hereafter, we use the following expression;  $\psi_{k_i k_j}^{C'}(x_i, x_j) = e^{i(2/3)k_{ij}r_{ij}} \phi_{k_{ij}}(r_{ij})$ . Notice that the numerical factor “2/3” in the exponential function is important [6, 7].

$$N^{(3\pi^-)} = \frac{1}{6} \prod_{i=1}^3 \int \rho(x_i) d^3 x_i \left| \sum_{j=1}^6 A(j) \right|^2, \quad (2.8)$$

where

$$\begin{aligned} A(1) &= A_1 = \psi_{k_1 k_2}^{C'}(x_1, x_2) \psi_{k_2 k_3}^{C'}(x_2, x_3) \psi_{k_3 k_1}^{C'}(x_3, x_1), \\ A(2) &= A_{23} = \psi_{k_1 k_2}^{C'}(x_1, x_3) \psi_{k_2 k_3}^{C'}(x_3, x_2) \psi_{k_3 k_1}^{C'}(x_2, x_1). \end{aligned} \quad (2.9)$$

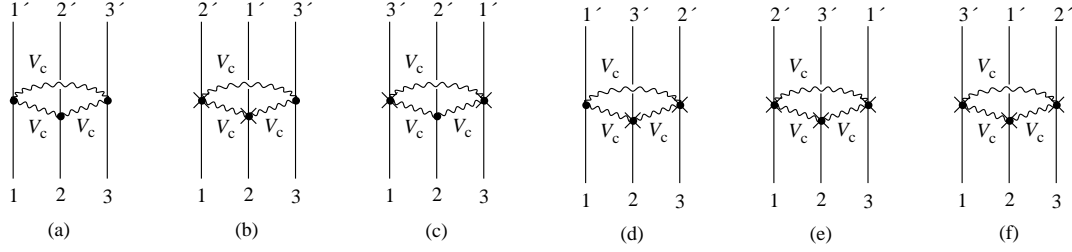


**Figure 3:** Diagrams of the 3rd order BEC for  $A(1) \sim A(6)$ .

$A_{ijk}$  is reflecting the permutations of particles,  $i, j, k$  in Fig. 3: Therein  $A(3) = A_{12}$ ,  $A(4) = A_{123}$ ,  $A(5) = A_{132}$  and  $A(6) = A_{13}$ . In the plane wave approx., we have the correct expression, where  $A(3) \sim A(6)$  are skipped [5, 7],

$$\begin{aligned} A(1) &= A_1 \xrightarrow{\text{PW}} e^{i(2/3)(k_{12} \cdot r_{12} + k_{23} \cdot r_{23} + k_{31} \cdot r_{31})} = e^{i(k_1 \cdot x_1 + k_2 \cdot x_2 + k_3 \cdot x_3)}, \\ A(2) &= A_{23} \xrightarrow{\text{PW}} e^{i(2/3)(k_{12} \cdot r_{13} + k_{23} \cdot r_{32} + k_{31} \cdot r_{21})} = e^{i(k_1 \cdot x_1 + k_2 \cdot x_3 + k_3 \cdot x_2)}. \end{aligned} \quad (2.10)$$

Combining  $A(1) \sim A(6)$  in Fig. 3, we obtain  $F_1$  as: (The other formulae  $F_{12} \sim F_{123}$  and  $F_{132}$  are given in [6, 7].)

$$F_1 = \frac{1}{6} [A_1 A_1^* + A_{12} A_{12}^* + A_{23} A_{23}^* + A_{13} A_{13}^* + A_{123} A_{123}^* + A_{132} A_{132}^*]. \quad (2.11)$$

$$\begin{aligned} \frac{N^{3\pi^-}}{N^{BG}} &= C \prod_{i=1}^3 \int \rho(x_i) d^3 x_i \left[ F_1 + 3\lambda F_{12} + 2\lambda^{\frac{3}{2}} \text{Re}(F_{123}) \right] \\ &= \frac{C}{(2\sqrt{3}\pi R^2)^3} \int d^3 \zeta_1 d^3 \zeta_2 \exp \left[ -\frac{1}{2R^2} \left( \frac{1}{2} \zeta_1^2 + \frac{2}{3} \zeta_2^2 \right) \right] \left[ F_1 + 3\lambda F_{12} + 2\lambda^{\frac{3}{2}} \text{Re}(F_{123}) \right] \end{aligned} \quad (2.12)$$

where  $\zeta_1 = x_2 - x_1$ ,  $\zeta_2 = x_3 - (m_1 x_1 + m_2 x_2)/M_2$ ,  $\zeta_3 = (m_1 x_1 + m_2 x_2 + m_3 x_3)/M$ ,  $M_2 = m_1 + m_2$  and  $M = m_1 + m_2 + m_3$ .

Finally, it is known that the core-halo model is a useful model. However, explicit expressions are skipped here. See our studies in [4, 5, 6, 7]. See also [8].

### 3. Analyses of data by STAR Coll and PHENIX Coll

**3-1)** For Coulomb corrected data, we employ the conventional formulae, Eqs. (2.1) and (2.2). Ours are given in Table 2 and Fig. 4. It is interesting that  $R_{2\pi} \sim R_{3\pi} \sim 8.5$  fm for data by STAR Coll.

**Table 2:** Analyses of corrected data by STAR and PHENIX Coll (Eqs. (2.1) and (2.2).)

	STAR			PHENIX		
	$R$ [fm]	$\lambda$	$\chi^2/\text{n.d.f.}$	$R$ [fm]	$\lambda$	$\chi^2/N_{dof}$
$2\pi^-$	$8.75 \pm 0.31$	$0.58 \pm 0.02$	23.0/25	$4.77 \pm 0.04$	$0.39 \pm 0.01$	178/40
$3\pi^-$	$8.26 \pm 0.39$	$0.50 \pm 0.02$	1.88/35	$6.92 \pm 0.82$	$0.34 \pm 0.10$	6.5/14

**3-2)** Corrected data with  $q_3 > 0.02$  GeV by PHENIX Coll are analyzed by conventional formula / LO approach. Our results are shown in Figs. 4 and 5, and Tables 2 and 3.

**3-3)** Raw data with  $q_3 > 0.02$  GeV are analyzed by the formulae of Coulomb wave function (Eqs. (2.6) and (2.12)). Our results are also shown in Fig. 6 and lower-part of Table 3.

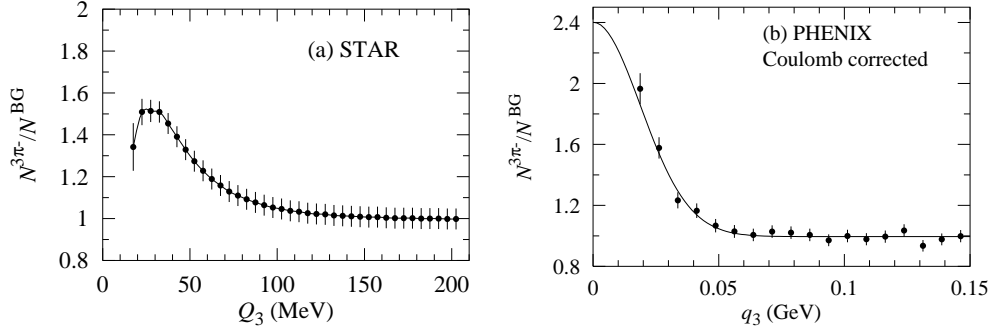


**Figure 4:** Analyses of corrected data by STAR Coll. and PHENIX Coll. Eqs. (2.1) and (2.2) are used.

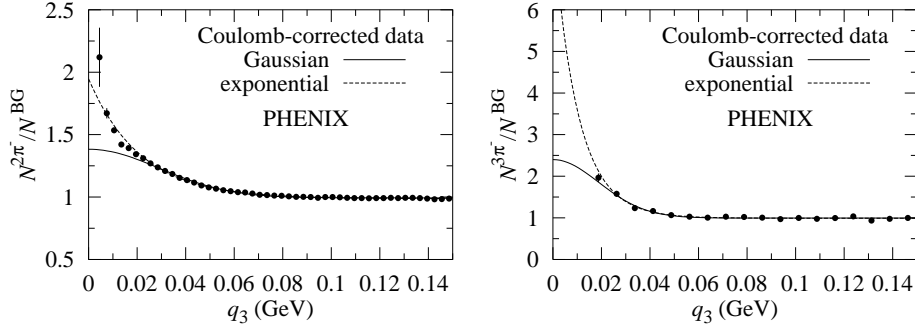


**Figure 5:** Corrected data are analyzed by Eq. (2.3) and (2.4)

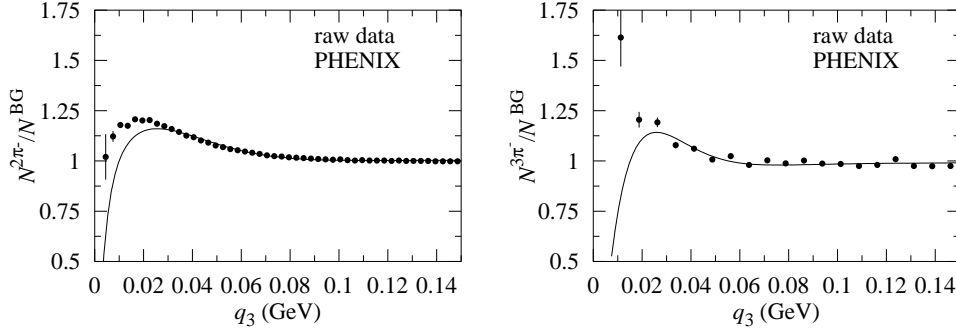


**Figure 6:** Analyses of raw data by PHENIX Coll. Eqs. (2.6) and (2.12) are used.

**3-4)** Using two formulae in the core-halo approach (with Gaussian source function, the fraction of core part  $f_c$  and the degree of coherent  $p_c$  in [5, 6, 7]) we obtain Fig. 7. In raw data, there is no over-lapping region. On the other hand, in corrected data, we observe very narrow over-lapping region. The reason of the wide region of  $3\pi$  BEC is due to large error bars of corrected data [2].

#### 4. Summary

**4-1)** From raw data as well as Coulomb corrected data in Au+Au at 130 GeV by STAR Coll., we get the following interaction ranges  $R_{2\pi} = 8.7$  fm and  $R_{3\pi} = 8.3$  fm, and can estimate

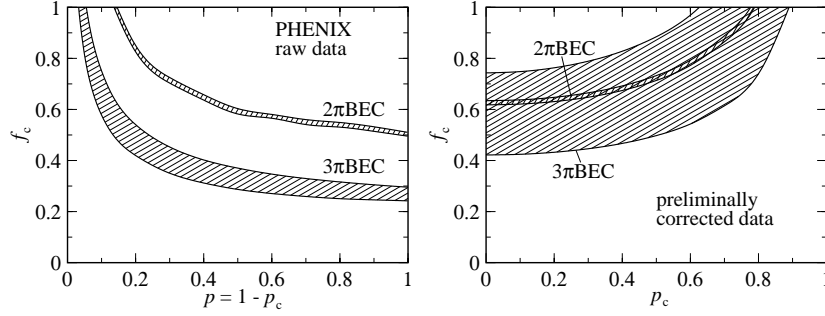
$$V = R_{3\pi}^3 \sim 500 \text{ fm}^3. \quad (4.1)$$

This value is compared with that of ALICE Coll [9],  $V = R_{\text{long}}R_{\text{out}}R_{\text{side}} \sim 300 \text{ fm}^3$  at  $dN_{ch}/d\eta = 1500$  and  $k_T \sim 0.3$  GeV in Pb+Pb at 2.76 TeV.

**4-2)** On the contrary, from corrected data at 200 GeV by PHENIX Coll., we obtain the ranges, by utilizing Eqs. (2.1) and (2.2),  $R_{2\pi} = 4.8$  fm ( $\lambda = 0.39$ ) and  $R_{3\pi} = 6.9$  fm ( $\lambda = 0.34$ ). From raw

**Table 3:** Analyses of data by PHENIX Coll. Eqs. (2.3), (2.4), (2.6) and (2.12) are used.

$E_{2B}$		$R$ [fm]	$p$	$c$	$\chi^2/N_{dof}$
$2\pi$	Gaussian	$6.58\pm 0.05$	$0.23\pm 0.00$	$0.98\pm 0.00$	156/40
	Exponential	$9.54\pm 0.16$	$0.99\pm 0.01$	$0.99\pm 0.00$	56/40
$3\pi$	Gaussian	$9.76\pm 1.11$	$0.24\pm 0.08$	$0.99\pm 0.00$	7.2/14
	Exponential	$14.36\pm 2.10$	$1.00\pm 0.07$	$0.99\pm 0.02$	6.3/14
raw data		$R$ (fm)	$\lambda$	$c$	$\chi^2/N_{dof}$
$2\pi$	Eq. (2.6)	$3.77\pm 0.03$	$0.253\pm 0.004$	$1.00\pm 0.00$	129/40
$3\pi$	Eq. (2.12)	$5.77\pm 0.32$	$0.19\pm 0.02$	$1.00\pm 0.00$	84/14

**Figure 7:** Analyses of data by core-halo model.

data, we have smaller interaction ranges  $R_{2\pi} = 3.8$  fm and  $R_{3\pi} = 5.8$  fm. The interaction ranges of data at 200 GeV by PHENIX Coll. are smaller than those of STAR Coll. At present, it is difficult to draw concrete physical picture for Au+Au collision at 200 GeV. Then we are waiting for final empirical analyses by PHENIX Coll.

**4-3)** Moreover, we also eager for empirical analyses of  $(2\pi^+)\pi^-$  and  $(2\pi^-)\pi^+$  combinations at RHIC and LHC energies. See [10, 11].

## References

- [1] J. Adams *et al.* [STAR Collaboration], Phys. Rev. Lett. **91**, 262301 (2003).
- [2] M. Csanad [PHENIX Collaboration], Nucl. Phys. A **774**, 611 (2006).
- [3] M. Biyajima, A. Bartl, T. Mizoguchi, O. Terazawa and N. Suzuki, Prog. Theor. Phys. **84**, 931 (1990) [Addendum-ibid. **88**, 157 (1992)].
- [4] T. Mizoguchi and M. Biyajima, Phys. Lett. B **499**, 245 (2001)
- [5] M. Biyajima, M. Kaneyama and T. Mizoguchi, Phys. Lett. B **601**, 41 (2004).
- [6] M. Biyajima, T. Mizoguchi and N. Suzuki, Phys. Lett. B **637**, 64 (2006).
- [7] M. Biyajima, T. Mizoguchi and N. Suzuki, AIP Conf. Proc. **828**, 589 (2006).
- [8] T. Csorgo, B. Lorstad, J. Schmid-Sorensen and A. Ster, Eur. Phys. J. C **9**, 275 (1999).
- [9] K. Aamodt *et al.* [ALICE Collaboration], Phys. Lett. B **696**, 328 (2011).
- [10] M. Biyajima, T. Mizoguchi and N. Suzuki, Phys. Lett. B **568**, 237 (2003).
- [11] P. Abreu *et al.* [DELPHI Collaboration], Phys. Lett. B **355**, 415 (1995).